doi:10.1510/icvts.2008.200006

INTERACTIVE CARDIOVASCULAR AND THORACIC SURGERY

Interactive CardioVascular and Thoracic Surgery 9 (2009) 301–308

www.icvts.org

ESCVS article - Valves

Computational fluid dynamics simulation of transcatheter aortic valve degeneration☆,☆☆

Harry A. Dwyer[a], Peter B. Matthews[b], Ali Azadani[b], Nicolas Jaussaud[b], Liang Ge[b], T. Sloane Guy[b], Elaine E. Tseng[b,*]

[a]*Department of Mechanical and Aeronautic Engineering, University of California at Davis, USA*
[b]*Department of Surgery, University of California at San Francisco Medical Center (UCSF) and San Francisco Veterans Affairs Medical Center (SFVAMC), San Francisco, CA, USA*

Received 4 December 2008; received in revised form 12 April 2009; accepted 15 April 2009

Abstract

Objectives: Studied under clinical trials, transcatheter aortic valves (TAV) have demonstrated good short-term feasibility and results in high-risk surgical patients with severe aortic stenosis. However, their long-term safety and durability are unknown. The objective of this study is to evaluate hemodynamic changes within TAV created by bioprosthetic leaflet degeneration. **Methods**: Computational fluid dynamics (CFD) simulations were performed to evaluate the hemodynamics through TAV sclerosis (35% orifice reduction) and stenosis (78% orifice reduction). A three-dimensional surface mesh of the TAV within the aortic root was generated for each simulation. Leaflets were contained within an open, cylindrical body without attachment to the sinus commissures representing the stent. A continuous surface between the annulus and TAV excluded the geometry of the native calcified leaflets and prevented paravalvular leak. Unsteady control volume analysis throughout systole was used to calculate leaflet shear stress and total force on the TAV. **Results**: Sclerosis increased total force on the TAV by 63% (0.602–0.98 N). Advancement of degeneration from sclerosis to stenosis was accompanied by an 86% increase in total force (1.82 N) but only a 32% increase in peak wall shear stress on the leaflets. Of the total force exerted on the TAV, 99% was in the direction of axial flow. Shear stresses on the TAV were greatest during peak systolic flow with stress concentrations on the tips of the leaflets. In the normal TAV, the aortic root geometry and physiologic flow dominate location and magnitude of shear stress. Following leaflet degeneration, the specific geometry of the stenosis dictates the profile of axial velocity leaving the TAV and shear stress on the leaflets. A dramatic increase in peak leaflet shear stress was observed (115 Pa stenosis vs. 87 Pa sclerosis and 29 Pa normal). **Conclusions**: CFD simulations in this study provide the first of its kind data quantifying hemodynamics within stenosed TAV. Stenosis leads to significant forces of TAV during systole; however, diastolic forces predominate even with significant stenosis. Substantial changes in peak shear stress occur with TAV degeneration. As the first implanted TAV begin to stenose, the authors recommend watchful examination for device failure.

Keywords: Aorta; Bioengineering; Valve disease

ESCVS Article

1. Introduction

Current transcatheter aortic valve (TAV) prototypes have been developed as a minimally invasive treatment for high-risk patients not suitable for surgical aortic valve replacement. TAV implantation in patients with severe aortic stenosis has shown excellent short-term procedural outcomes [1–3]. Acutely, transvalvular gradients are substantially reduced, valve area is increased, and ejection fraction is improved. Alain Cribier, who performed the first in man TAV procedure in 2002, has reported excellent mid-term follow-up results, including two patients with stable aortic valve area (1.64 cm^2) and mean aortic gradient (12 mmHg) at 24 months postoperatively [4]. These clinical successes may prompt physicians to consider TAV as a less invasive treatment for younger, healthier patients who would traditionally be candidates for surgical aortic valve replacement. However, patients currently receiving TAV have relatively short life expectancies, and thus it is unlikely that present studies will yield data about long-term device durability.

Current TAV contain bioprosthetic leaflets, which are subject to structural deterioration over time. Over 20 years, 20–30% of surgically implanted bioprostheses with pericardial valves must be explanted, primarily due to structural valve deterioration. Degeneration occurs more rapidly in young patients, and the rate of failure accelerates exponentially 10 years after AVR; patients age 50 years have twice the probability of explant (60% vs. 30%) as those 10 years older [5]. Such failure would also be expect-

☆ Presented at the 57th International Congress of the European Society for Cardiovascular Surgery, Barcelona, Spain, April 24–27, 2008.

☆☆ Support for this work has been provided by the American Heart Association Beginning Grant-in-Aid 0565148Y (Burlingame, CA) and the Northern California Institute for Research and Education (San Francisco, CA).

*Corresponding author. UCSF Medical Center, Division of Cardiothoracic Surgery, 500 Parnassus Avenue, Suite W405, Box 0118, San Francisco, CA 94143-0118, USA. Tel.: +1-415-353-8195; fax: +1-415-353-1312.

E-mail address: Elaine.tseng@ucsfmedctr.org (E.E. Tseng).

ed of TAV if the technology's indications are expanded to younger patients.

In this investigation we have developed a simulation of flow through TAV using computational fluid dynamics (CFD). The unique geometry of TAV likely yields different hemodynamics from that of surgically implanted prostheses. CFD simulations were used to quantify the spatial gradient of the blood pressure during ejection, the resulting force acting on the prosthesis, as well as the wall shear stress on the TAV. Since the TAV bioprosthetic leaflets will gradually degenerate and stenose, we hypothesize an incurring change in hemodynamics that could potentially accelerate leaflet degeneration, reduce prosthetic stability, or cause hemostatic abnormalities. The transvalvular pressure gradient developing from a decrease in effective orifice area will create a substantial systolic ejection force. Unlike surgically sutured bioprostheses, ejection force may dislodge the TAV similar to distal migration of an abdominal aortic stent graft.

2. Materials and methods

2.1. Mesh generation

For the CFD simulation, a rigid surface mesh was generated to represent the geometry of a TAV implanted within the aorta. Fluid flows through the modeled aorta, which extends from the annulus to the proximal descending aorta (Fig. 1). The sinus is a symmetric approximation of human anatomic dimensions; this geometry has been used in previous computational simulation of blood flow through the aortic valve [6]. The relevant dimensions are aortic valve radius (12 mm), sinus depth (5.75 mm), and sinus height (21 mm). The aortic arch is modeled as a simple curved pipe. Prior CFD simulations have indicated that aortic root geometry has a negligible effect on flow distal to the ascending aorta, justifying this simplification [7]. Within the root is a second mesh estimating the geometry of current TAV design [8], an open cylinder with an internal diameter of 24 mm representing free standing leaflets within the stent. An illustration of a TAV implanted in a stenotic root is presented in Fig. 2. During systole the leaflets open to the stent, forming the open cylinder; the stent itself is assumed to have a negligible effect on flow, and thus is excluded. However, because the leaflets are within a stent, they have no attachment to the commissures of the aorta (Fig. 2). Finally, the TAV mesh is merged to the aortic mesh at the annulus, creating a contiguous boundary and preventing any paravalvular leak to the left ventricle.

Following the initial simulation, two additional TAV meshes were created to simulate 1) aortic sclerosis, a 35% reduction in orifice area (2.93 cm^2); and 2) aortic stenosis, a 78% reduction in orifice area (1 cm^2). No data are yet available on structural degeneration of TAV, so the geometry of stenosis had to be estimated. In a classic study, Thubrikar et al. showed that degenerative calcification of bioprostheses is initiated in the region of leaflet flexion where tissue is exposed to the greatest mechanical stress, a result also observed in vitro [9, 10]. We, therefore, predict that calcification will develop on the epipericardial

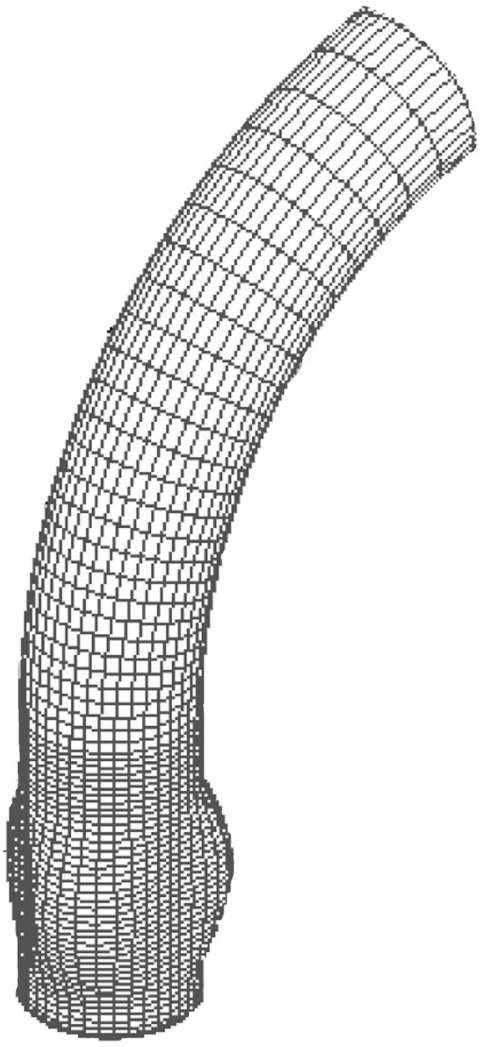

Fig. 1. Surface mesh of the aorta, extending from the annulus to proximal aortic arch.

(aortic) surface of each TAV leaflet, preventing complete opening of the valve leaflets. This pattern would lead to an asymmetric reduction in orifice area. The desired effective orifice area was created by simulating individual leaflet degeneration, where three points 120° apart were brought toward the center of the cylinder (Fig. 3).

2.2. Computational fluid dynamics (CFD)

The loading conditions applied to the mesh were taken from literature, representative of normal aortic pressure (120/80 mmHg) [11]. The CFD methodology utilized in this study has previously proven its efficacy characterizing flow in the aortic arch and bifurcations [7]. This approach requires a detailed, three-dimensional and time-dependent description of flow through the aortic valve. The simulation is driven by a system of fluid flow equations known as the Navier–Stokes equations, which for an incompressible fluid in dimensionless control volume form are:

$$\iint_S \vec{V} \cdot d\vec{A} = 0 \qquad \text{Continuity} \tag{1}$$

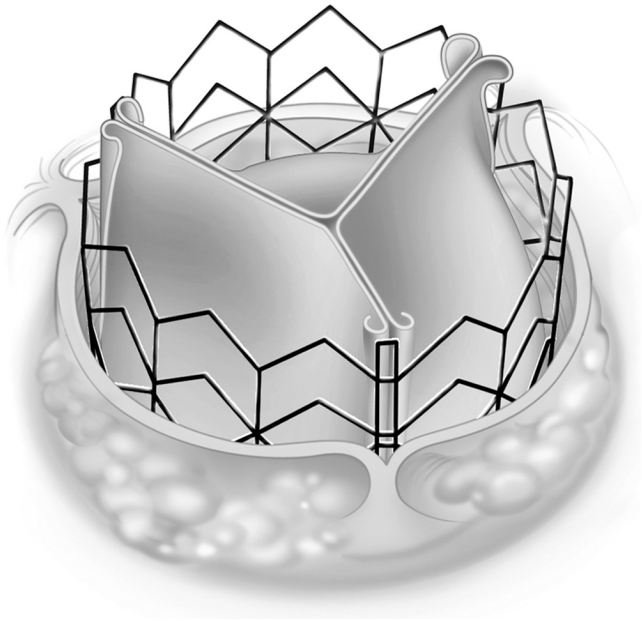

Fig. 2. Illustration of an implanted TAV.

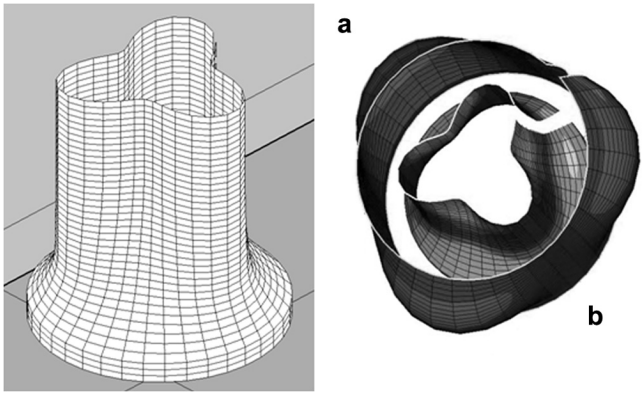

Fig. 3. (a) Surface mesh of TAV sclerosis. Orifice area has been reduced by 35%; (b) sclerotic TAV within the aortic sinus. The separation of the two meshes is shown for clarity.

$$\frac{\alpha^2}{\mathrm{Re}}\int\int\int_v \frac{\partial \vec{V}}{\partial t}dV+\int\int\int_v(\vec{V}\cdot\vec{\nabla})\vec{V}\,dV$$

$$=-\int\int_s p\cdot d\vec{A}+\frac{1}{\mathrm{Re}}\int\int_s \bar{\bar{\tau}}\cdot d\vec{A} \qquad \text{Momentum} \qquad (2)$$

where p is the pressure, $\bar{\bar{\tau}}$ is the viscous stress tensor, $\mathrm{Re}=\frac{2R\bar{U}}{\nu}$ is the Reynolds number, $\alpha=R\left(\frac{\omega}{\nu}\right)^{1/2}$ is the Womersley parameter, R is the inlet radius of the aorta, $\bar{U}$ is the maximum inlet velocity, ν is the kinematic viscosity of the fluid, and ω is the inlet pulse frequency ($\omega=2\pi f$ where f is the heart rate). Blood flowing through the aorta is modeled as a Newtonian fluid, standard for CFD simulations of arterial flow, using ~600,000 finite elements [12]. Computational evaluations are made at discrete time intervals; one heart cycle requires 320 computational steps per second. Values for the maximum velocity and flow area are:

$$U_{\max}=60\ \text{cm/sec}\quad A_{flow}=\pi r^2\quad r=1.2\ \text{cm}$$

$$A_{flow}=4.52\times10^{-4}\ \text{m}^2 \qquad (3)$$

The total force on the aortic valve is obtained by performing an unsteady control volume analysis around the outer surface of the valve equivalent to the force necessary to hold the valve on the root [13]. There are four contributions to the force, and they are the following: (1) the fluid momentum flux at the inlet and exit of the valve; (2) the unsteady change of momentum in the valve control volume; (3) the dynamic pressure force on the valve; and (4) the viscous shear stresses on the outer wall of the valve. Total force was made dimensionless, allowing a good estimation of force to be made over a significant Reynolds number and size range. However, force is presented in Newtons for the specific geometries used.

The dimensionless force coefficient, C_{force}, is defined as

$$C_{force}=\frac{Force_{real}}{\rho U_{\max}^2 A_{flow}} \quad \text{where} \quad \rho-\text{fluid density}$$

$$U_{\max}-\text{Maximum flow velocity} \qquad (4)$$

The values of pressure and shear stress in the figures have also been made dimensionless in the following manner

$$p=\frac{p_{dynamic}}{\rho\left(\frac{U_{\max}}{2}\right)^2} \qquad \tau=\frac{\tau_{real}}{\mu\frac{U_{\max}}{Diameter}}$$

and

$$\rho\left(\frac{U_{\max}}{2}\right)^2=90\ \text{Pa}\ \text{ and }\ \mu\frac{U_{\max}}{Diameter}=0.084\ \text{Pa} \qquad (5)$$

3. Results

3.1. TAV hemodynamics

Results of the simulation yield ~300 ms of systolic flow through the TAV; peak flow occurs at ~160 ms following the beginning of unsteady flow. The normal, unstenosed TAV creates a converging jet flow distal to the valve. A high velocity stream in the center of the lumen of the ascending aorta is created, with maximum axial velocity of ~147 cm/s (Fig. 4a). However, because the total lumen area increases in the ascending aorta, average velocity decreases. Velocity fields through the aortic arch are essentially identical to those within a simple curved pipe mesh without addition of the aortic root geometry, suggesting that implantation of the TAV has a negligible effect on hemodynamics downstream of the ascending aorta. Instead, the Womersley parameter, sensitive to changes in heart rate, dominates the profile of flow within the arch. Fig. 4a

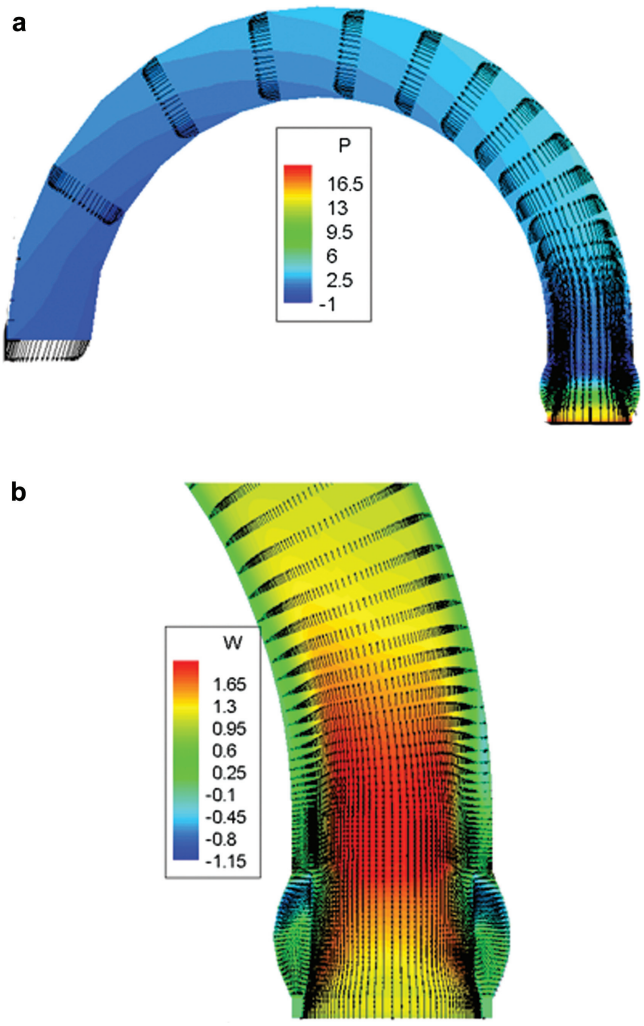

Fig. 4. Flow through normal TAV: (a) velocity vectors and dynamic pressure contours at peak acceleration; (b) velocity vectors and vertical velocity profiles at peak flow.

presents a profile view of velocity vectors and dynamic pressure contours at peak fluid acceleration. This illustrates the gradient of pressure at the TAV, the complex jet flow immediately distal, and the unaffected pressure and velocity profiles in the arch.

Flow at the level of the TAV and aortic root is dominated by the geometry of the TAV and to a lesser extent that of the sinus. The volume of the sinus cavity is fixed because this simulation does not portray moving leaflets of the TAV nor dynamic root expansion. Thus, the net flow of the incompressible fluid into or out of the sinus must be zero. There are nonetheless complex, unsteady flows in the sinus cavity due to entrainment of fluid in the sinus. Blood is recirculated locally at the valve tip; blood leaving the sinus along the aortic face of the TAV leaflet pulls new blood into the sinus from near the aortic root wall creating regions of both positive and negative axial flow (Fig. 4b). In this figure, color contours represent the profile of the velocity field, not the pressure field as in Fig. 4a; i.e. red represents the greatest magnitude of velocity in the positive axis of the aortic root. Vectors represent the direction and magnitude of fluid velocity.

3.2. Stenosis hemodynamics

Results of CFD simulations of the stenotic TAV are similar qualitatively to that of the normal prosthesis, but with quantitative differences. The sinus and TAV geometry was shown in the previous simulation to have a negligible effect on aortic arch hemodynamics. The further reduction of orifice area created by TAV stenosis increases fluid velocity distal to the prosthesis, but velocity profiles and pressure gradients in the arch are largely unaffected (Fig. 5a). Stenosis of the TAV does, however, greatly alter the flow in and around the stent, creating significant gradients of both velocity and pressure in the aortic root. Even at aortic sclerosis, the maximum flow velocity has increased approximately 60% from the maximum flow velocity in the normal TAV (Fig. 5b). Fluid entrainment into the sinus remains, generating similar vortical flows and recirculating blood

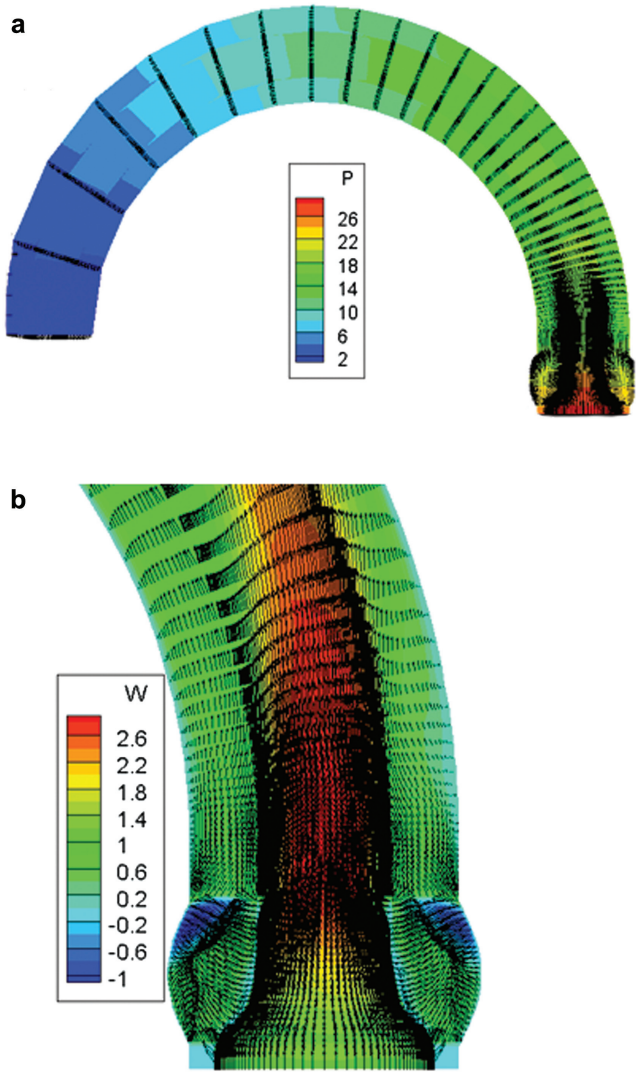

Fig. 5. Flow through stenotic TAV: (a) velocity vectors and dynamic pressure contours at peak acceleration; (b) velocity vectors and vertical velocity profiles at peak flow.

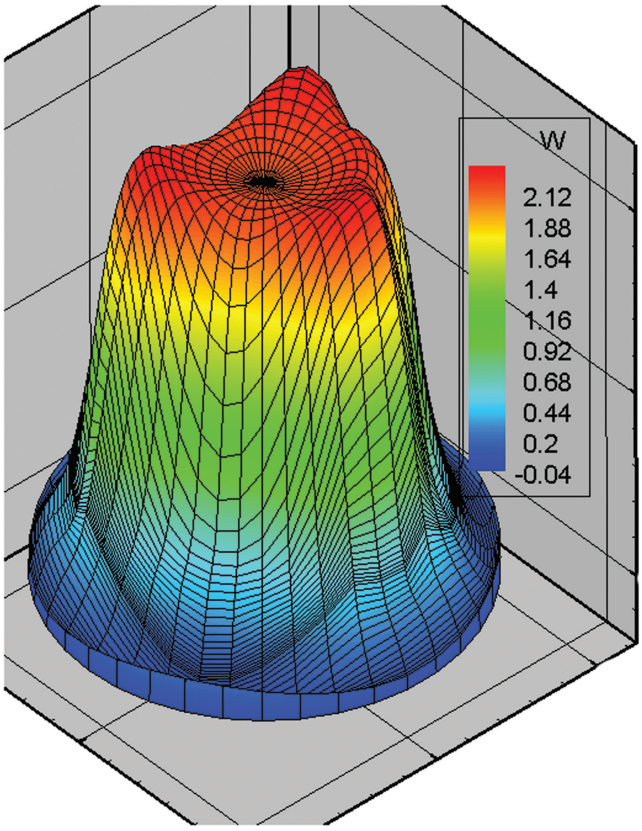

Fig. 6. Axial velocity profile at peak flow immediately distal to a sclerotic TAV.

around the leaflet tips. The specific geometry of the stenosis appears to be the dominating factor in the profile of axial fluid velocity leaving the TAV (Fig. 6). Clinically, the shape of a diseased aortic valve can vary significantly from patient to patient; thus, the profile of fluid velocity entering the ascending aorta will vary greatly as well. Nonetheless, the generalized blockage effect shown in the paper captures important hemodynamic features of the stenosis.

3.3. Wall shear stress

The profile of wall shear stress on the leaflets of the open TAV has been examined, as well as the magnitude or absolute value of the total wall shear stress (Fig. 7). Peak shear stress occurs near the tip of the leaflets, and peaks during maximum flow through the valve, an observation seen in both the root and the aortic arch [7]. Although the normal TAV is a simple open cylinder, there is an asymmetric profile of wall shear stress on the leaflets, indicating that the sinus geometry and fluid entrainment are largely responsible. At initial implantation, stress during peak flow is in the range of 8–18 Pa. Maximum stress occurs at the location of fluid recirculation into the sinus, the tip of the TAV, reaching a value of 29 Pa. Stenosis of the TAV dramatically increases average and peak wall shear stress during systole. The geometry of the calcified leaflets not the sinus geometry is now the dominating factor determining the

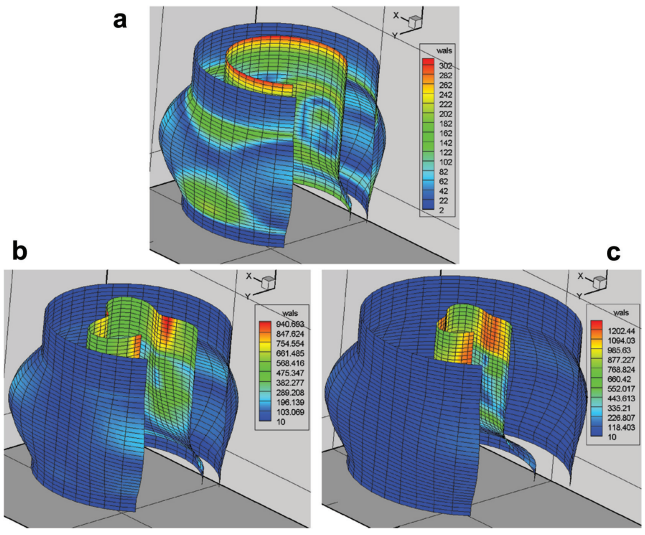

Fig. 7. Comparison of wall shear stress in a TAV: (a) normal; (b) sclerotic; and (c) stenosed.

profile and magnitude of wall shear stress. In the sclerotic TAV shear stress on the leaflets is in the range of 30–50 Pa. Progressing to severe stenosis causes a much smaller increase in average wall shear stress, ~40–60 Pa. In both simulations peak stress now occurs at the region of greatest stenosis again at the tip of the TAV leaflets. Unlike average stress, peak wall shear stress continues to increase dramatically, reaching 87 Pa for TAV sclerosis and 115 Pa for severe stenosis.

3.4. Ejection force

An estimation of the total force exerted on the TAV may be important for predicting device failure. Total force presented here is the magnitude of force in all three axes, but 99% of this value is in the direction of flow. By far, the pressure gradient created by the reduction of orifice area is the largest component contributing to total force. For all models, total force peaks during maximum flow. This force reaches 0.98 Newtons for TAV sclerosis and 1.82 Newtons for severe stenosis (Fig. 8). To put the magnitude of force in perspective, a gross estimation of retrograde force on the TAV during diastole can be easily calculated. Given an average diastolic gradient of 80 mmHg and the total in-plane surface area of the closed TAV, the total force is ~4.83 Newtons. While this is a rough estimate, it demonstrates that even severe stenosis of the leaflets creates an ejection force of one-third of the normal diastolic load.

4. Discussion

Simulation with CFD has shown to be a useful tool for quantifying TAV hemodynamics and the effect of bioprosthetic leaflet stenosis on flow. The impact of the TAV, either normal or stenosed, on flow in the aortic arch is negligible. However, aortic root hemodynamics are significantly altered by stenosis. The specific geometry of the leaflet stenosis appears to dominate the profile of axial velocity

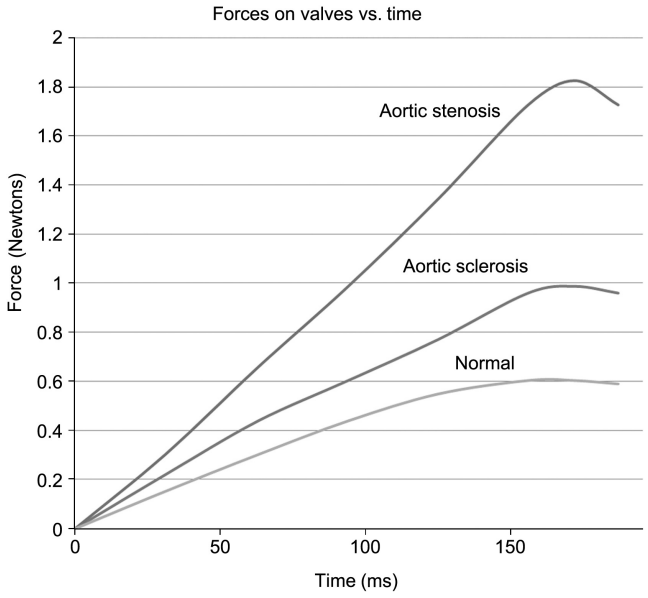

Fig. 8. Ejection force on normal, sclerotic, and stenosed TAV.

leaving the TAV and shear stress on the leaflets. Advancement of TAV degeneration from sclerosis to stenosis is accompanied by an 86% increase in total force acting to eject the device and a 32% increase in peak wall shear stress on the leaflets.

4.1. Flow through aortic valves prostheses

The presented simulation has not been validated experimentally, and thus a comparison with hemodynamic measures in literature is important. Our calculations of TAV flow show many similarities with in vitro studies of normal and bioprosthetic aortic valves. As compared to the peak velocity 147 cm/s in TAV, flow through stented bioprosthesis reaches 200–300 cm/s, which dissipates shortly distal. Flow through non-stented bioprosthesis and native aortic valves are 125–200 cm/s and 135 cm/s, respectively [14]. Consistent with TAV, computational analyses of surgical bioprostheses have shown complex fluid interaction at the leaflet tips and a recirculating zone of vortical flow in the sinus [15]. This flow is thought to be important for aiding coronary flow and fast, efficient valve closure. Finally, the effect of stenosis geometry has been examined in a pulse duplicator study. When aortic valve leaflets were obstructed with silicone rubber, the specific orifice shape dictated the velocity of axial velocity 25 mm distal to the valve [16].

Overall, measurements of wall shear stress in our model of the TAV were higher than that seen for aortic valves in literature. Weston et al. found asymmetric distribution of shear stress on polymeric leaflets within an acrylic aortic root, consistent with the TAV; greatest shear stress was at the tips of the leaflets. They reported a peak of ~8 Pa, slightly lower than our measurements of average stress on the TAV leaflets but considerably less than our calculated peak stress [17]. Wall shear stress on the normal TAV was, however, lower than that measured for mechanical prostheses. Two tilting disc valves created wall shear of 30–50 Pa during systole in a pulse duplicator [18]. In order to simulate the effect of stenosis, Stevenson et al. modeled the aortic valve as a hollow cylinder, similar to the geometry we have used, but then created stenosis with an axisymmetric reduction in diameter. A cylindrical orifice size of 1.1 cm^2 resulted in a peak wall shear stress of 82 Pa [19]. Although this is still less than our calculation of 115 Pa, it is important to note that TAV stenosis is not cylindrically shaped, creating areas of concentrated high shear stress.

4.2. TAV orientation

One important observation of this study is that the sinus cavity helps to direct flow leaving the TAV. Unique among bioprosthetic aortic valves, TAV have a free axis of rotation within the annulus at the time of implantation. Minimally invasive, transcatheter delivery creates the possibility of malalignment between TAV leaflets and the aortic root sinus. Vortical sinus flow similar to that seen in this model plays an important role in efficient closure of native and surgical bioprosthetic valve leaflets [14, 20]. Altering the valve's kinematics may have implications on the long-term durability of the prosthesis. Pericardial tissue leaflet stress is directly correlated with calcification and tissue failure; degeneration appears at the sites of large flexure strains [9, 10]. Durability will be a critical issue for percutaneous heart valves should the technology become available to a larger patient population in the future [21]. Similar to their surgical counterparts, increasing the lifespan of TAV will likely be dependent on improving the valve's ability to function normally within the root and reducing concentrations of stress [22]. Incorrect orientation of the TAV within the annulus could create irregular leaflet kinematics and accelerate structural degeneration. Future work investigating the relationship of TAV orientation on flow would require a full fluid-structure interaction model, but is important for evaluating the sensitivity of valve function to correct alignment with the sinus.

4.3. Hemodynamic disturbances

The effect of stenosis of the native aortic valve on platelet and blood cell injury and the formation of thrombus has been studied experimentally and observed clinically. Aortic valve stenosis is associated with bleeding episodes due to acquired type 2A von Willebrand syndrome. In one clinical study, high shear stress due to reduced effective orifice area led to platelet-function abnormalities, decreasing blood concentration of large von Willebrand factor multimers and collagen-binding activity [23]. These abnormalities were present in 67–92% of patients with severe aortic stenosis, and the magnitude of hematologic abnormality was significantly correlated with the mean transvalvular gradient [23]. Experimental evidence has also shown that red cells and platelets are susceptible to damage under conditions of high shear stress in blood vessels [24]. Damaged blood elements are powerful activators of thrombus formation, which could occur in flow stagnations or eddies formed around the stainless steel stent of TAV. Our measurements of peak shear stress during sclerosis are within

the range of platelet and cell injury, albeit briefly, and both average and peak shear stress during severe stenosis are well within this range.

4.4. Stent migration

Migration is a known complication of stent grafts, such as abdominal aortic aneurysm stent grafts, and is potentially lethal for TAV. This study has shown that degenerative stenosis is accompanied by a very large increase in total force in the direction of axial flow. Compared to the normal TAV, ejection force increased 63% for a sclerotic TAV and 202% for a stenotic TAV. However, compared to the diastolic force acting to push the TAV into the left ventricle, ejection force is substantially less; even in severe stenosis the magnitude of ejection force is approximately one-third of normal diastolic force. Migration of TAV in either direction has rarely been seen clinically despite the high pressure gradient [4]. As an explanation, Walther et al. have proposed that the rigid, calcified annulus contributes to the stent's stability providing sufficient frictional force to prevent migration to the aorta or left ventricle [25]. In addition, the effect of TAV healing into the annulus or pannus growth into the TAV is yet to be determined, but will likely further secure the stent. At this time, the force required to cause acute failure of the TAV, such as migration, stent fracture or leaflet detachment, is unknown. However, given the initial stability of the TAV in the annulus and the results of this simulation, distal migration due to stenotic orifice restriction does not seem to be a concern.

4.5. Study limitations

One limitation of the CFD model is that systolic flow begins after an instantaneous opening of the valve; leaflets maintain a fixed position within the TAV through end-systole. Currently, the kinematics of TAV leaflet opening at the beginning of systole are unknown. We assume that the overall hemodynamics throughout systole, not the initial instantaneous flow, is most important. Additionally, measures of shear stress and total force reported at peak flow are unaffected by the short period of leaflet opening. It should nonetheless be mentioned that in vivo leaflet motion will displace fluid in the sinus, perhaps altering our model's simulation of sinus entrainment and shear on the aortic surface of the leaflets. Incorporating leaflet kinetics with a fluid-structure interaction model would improve upon this limitation and should be examined in the future.

5. Conclusions

Computational models and in vitro experiments have been implemented to study hemodynamics of the native and bioprosthetic aortic valve, but to our knowledge none for TAV. The fluid dynamics of TAV are similar to that of the native aortic valve and comparable to surgical bioprostheses. Although not validated experimentally, our simulation of flow is consistent with previous findings of prosthetic aortic valve function. Peak flow created in the TAV is slightly greater than the average native valve or non-stented bioprosthesis, but less than stented bioprostheses. In the normal TAV, there is a concentration of wall shear stress at the leaflet tips. Both average and maximum wall shear stress at peak flow exceed that measured in vitro for surgical bioprostheses, but are less than that of mechanical prostheses. Stenosis rapidly accelerates the magnitude of wall shear, reaching values that could be clinically relevant to hemolytic injury and thrombus deposition. Finally, although distal migration is a clinical hazard of stents in the abdominal aorta, TAV seem well seated in the calcified annulus. Considering their initial stability under the diastolic pressure gradient, ejection during systole is likely not a concern.

Glossary

t	Time
f	Heart rate
R	Radius
$d\vec{A}$	Area
dV	Volume
ρ	Fluid density
P	Dynamic pressure
μ	Viscosity
υ	Kinematic viscosity
$\overline{\overline{\tau}}$	Shear stress
$\vec{V}$	Fluid local velocity
$\overline{U}$	Mean velocity
U_{max}	Maximum velocity

References

[1] Bauer F, Eltchaninoff H, Tron C, Lesault PF, Agatiello C, Nercolini D, Derumeaux G, Cribier A. Acute improvement in global and regional left ventricular systolic function after percutaneous heart valve implantation in patients with symptomatic aortic stenosis. Circulation 2004;110:1473–1476.

[2] Cribier A, Eltchaninoff H, Tron C, Bauer F, Agatiello C, Sebagh L, Bash A, Nusimovici D, Litzler PY, Bessou JP, Leon MB. Early experience with percutaneous transcatheter implantation of heart valve prosthesis for the treatment of end-stage inoperable patients with calcific aortic stenosis. J Am Coll Cardiol 2004;43:698–703.

[3] Webb JG, Pasupati S, Humphries K, Thompson C, Altwegg L, Moss R, Sinhal A, Carere RG, Munt B, Ricci D, Ye J, Cheung A, Lichtenstein SV. Percutaneous transarterial aortic valve replacement in selected high-risk patients with aortic stenosis. Circulation 2007;116:755–763.

[4] Cribier A, Eltchaninoff H, Tron C, Bauer F, Agatiello C, Nercolini D, Tapiero S, Litzler PY, Bessou JP, Babaliaros V. Treatment of calcific aortic stenosis with the percutaneous heart valve: mid-term follow-up from the initial feasibility studies: the French experience. J Am Coll Cardiol 2006;47:1214–1223.

[5] Roselli EE, Smedira NG, Blackstone EH. Failure modes of the Carpentier–Edwards pericardial bioprosthesis in the aortic position. J Heart Valve Dis 2006;15:421–427; discussion 427–428.

[6] De Hart J, Peters GW, Schreurs PJ, Baaijens FP. Collagen fibers reduce stresses and stabilize motion of aortic valve leaflets during systole. J Biomech 2004;37:303–311.

[7] Shahcheraghi N, Dwyer HA, Cheer AY, Barakat AI, Rutaganira T. Unsteady and three-dimensional simulation of blood flow in the human aortic arch. J Biomech Eng 2002;124:378–387.

[8] Vahanian A, Alfieri OR, Al-Attar N, Antunes MJ, Bax J, Cormier B, Cribier A, De Jaegere P, Fournial G, Kappetein AP, Kovac J, Ludgate S, Maisano F, Moat N, Mohr FW, Nataf P, Pierard L, Pomar JL, Schofer J, Tornos P, Tuzcu M, van Hout B, von Segesser LK, Walther T. Transcatheter valve implantation for patients with aortic stenosis: a position statement from the European Association of Cardio-Thoracic Surgery (EACTS) and the European Society of Cardiology (ESC), in collaboration with the

European Association of Percutaneous Cardiovascular Interventions (EAPCI). Eur J Cardiothorac Surg 2008;34:1–8.
[9] Bernacca GM, Fisher AC, Wilkinson R, Mackay TG, Wheatley DJ. Calcification and stress distribution in bovine pericardial heart valves. J Biomed Mater Res 1992;26:959–966.
[10] Thubrikar MJ, Deck JD, Aouad J, Nolan SP. Role of mechanical stress in calcification of aortic bioprosthetic valves. J Thorac Cardiovasc Surg 1983;86:115–125.
[11] Mohrman D. Cardiovascular Physiology. New York: McGraw-Hill, 2006: 47–52.
[12] Berger SA, Goldsmith EW, Lewis ER. Introduction to Bioengineering. Oxford, UK: Oxford University Press, 2000:134–139.
[13] White FM. Fluid Mechanics. New York: McGraw-Hill, 2005:135–161.
[14] Yoganathan AP, He Z, Casey Jones S. Fluid mechanics of heart valves. Annu Rev Biomed Eng 2004;6:331–362.
[15] Nicosia MA, Cochran RP, Einstein DR, Rutland CJ, Kunzelman KS. A coupled fluid-structure finite element model of the aortic valve and root. J Heart Valve Dis 2003;12:781–789.
[16] Bluestein D, Einav S. The effect of varying degrees of stenosis on the characteristics of turbulent pulsatile flow through heart valves. J Biomech 1995;28:915–924.
[17] Weston MW, LaBorde DV, Yoganathan AP. Estimation of the shear stress on the surface of an aortic valve leaflet. Ann Biomed Eng 1999;27:572–579.
[18] Tillmann W, Reul H, Herold M, Bruss KH, van Gilse J. In-vitro wall shear measurements at aortic valve prostheses. J Biomech 1984;17:263–279.
[19] Stevenson DM, Yoganathan AP, Williams FP. Numerical simulation of steady turbulent flow through trileaflet aortic heart valves–II. Results on five models. J Biomech 1985;18:909–926.
[20] Yacoub MH, Kilner PJ, Birks EJ, Misfeld M. The aortic outflow and root: a tale of dynamism and crosstalk. Ann Thorac Surg 1999;68:S37–S43.
[21] Vassiliades TA Jr, Block PC, Cohn LH, Adams DH, Borer JS, Feldman T, Holmes DR, Laskey WK, Lytle BW, Mack MJ, Williams DO. The clinical development of percutaneous heart valve technology: a position statement of the Society of Thoracic Surgeons (STS), the American Association for Thoracic Surgery (AATS), and the Society for Cardiovascular Angiography and Interventions (SCAI) Endorsed by the American College of Cardiology Foundation (ACCF) and the American Heart Association (AHA). J Am Coll Cardiol 2005;45:1554–1560.
[22] Kim H, Lu J, Sacks MS, Chandran KB. Dynamic simulation pericardial bioprosthetic heart valve function. J Biomech Eng 2006;128:717–724.
[23] Vincentelli A, Susen S, Le Tourneau T, Six I, Fabre O, Juthier F, Bauters A, Decoene C, Goudemand J, Prat A, Jude B. Acquired von Willebrand syndrome in aortic stenosis. N Engl J Med 2003;349:343–349.
[24] Wurzinger LJ, Blasberg P, Schmid-Schonbein H. Towards a concept of thrombosis in accelerated flow: rheology, fluid dynamics, and biochemistry. Biorheology 1985;22:437–450.
[25] Walther T, Dewey T, Wimmer-Greinecker G, Doss M, Hambrecht R, Schuler G, Mohr FW, Mack M. Transapical approach for sutureless stent-fixed aortic valve implantation: experimental results. Eur J Cardiothorac Surg 2006;29:703–708.